Absolute Cross Sections for Single Ionization of Alkali Ions by Electron Impact. II. Na^+ and K^+ Results and Comparisons with Theory*

J. W. Hooper, W. C. Lineberger, and F. M. Bacon
Georgia Institute of Technology, Atlanta, Georgia
(Received 19 August 1965)

The absolute cross sections for single ionization of Na^+ and K^+ ions by electron impact have been measured over the electron-energy range from below threshold to 1000 eV. The measurements were performed in a crossed-beam facility operating under continuous-beam conditions. Numerous checks were performed to establish the validity of the data. For both Na^+ and K^+, the measured cross sections were zero below threshold, and thus no "correction" was required to obtain the actual cross section. The present Na^+ and K^+ data and the Li^+ data presented in the preceding paper are discussed and compared with relevant theory and experiment.

I. INTRODUCTION

In the preceding paper,[1] a crossed-beam apparatus for the investigation of the ionization of positive ions by electron impact was described. The measurement techniques were discussed, and results were presented for the single ionization of Li^+ ions by electron impact. In this paper absolute measurements of the cross sections for single ionization of Na^+ and K^+ ions by electron impact are presented for electron energies from below threshold to 1000 eV. The Li^+, K^+, and Na^+ data are discussed and compared to the relevant theoretical and experimental data which are available. In appendices an expression for the ionization cross section in a crossed-beam experiment is derived, and various beam-pulsing schemes are discussed.

II. K^+ RESULTS

The experimental apparatus and measurement technique is the same as that reported previously.[1] The source of K^+ ions is thermionic, and consists of a platinum-gauze filament coated with a potassium-alumino-silicate, Kingman feldspar. Upon heating to 1000°C, this material provides a copious source of K^+ ions. Mass analysis of the emitted ions indicates that at least 99% of the total ion emission consists of K^+ ions.

On the basis of classical estimates, it is expected that the K^+ ionization cross sections are 10 to 20 times larger than the corresponding Li^+ cross sections. Such a result was found, and, consequently, many of the stray currents, which were of the same magnitude as the ionization signal current in the Li^+ measurements,[1] now represented small corrections. Signal-to-background ratios of greater than 20 were easily obtained over most of the electron-energy range.

A number of cross-section measurements were made at electron energies below the threshold for formation of K^{++} ions (31.81 eV). The apparent cross sections were zero, to within the experimental error; in no cases did the below-threshold measurements yield apparent cross sections which were greater than 4% of the magnitude of the above-threshold measurements reported here.

The experimental procedures and checks employed in these measurements were the same as those used in the Li^+ measurements. In particular the variation of the measured cross sections with ion-beam intensity, electron-beam intensity, and form factor are substantially the same as that shown in Fig. 3, Ref. 1. The larger K^+ ionization cross section did, however, permit the use of smaller electron-beam intensities while still maintaining a workable signal-to-background ratio. Measurements were made throughout the entire electron energy range with electron beam intensities as low as 100 μA. The measured cross sections were independent of electron-beam intensity. Thus, for example, the measured cross sections at 1000-eV electron energy showed no significant change as the electron-beam intensity was increased from 100 μA to 4.0 mA. The ion-beam energy was also varied from 800 to 1500 eV; again no significant variation in the measured cross sections was observed.

The following are typical measurement data, for 500-eV electron energy and 1000-eV ion energy. The symbols for the various quantities are the same as those employed previously.[1]

$$I^+ = 2.00\times10^{-7}\ \text{A},$$
$$J = 1.00\times10^{-3}\ \text{A},$$
$$I^{++}(0,0) = +0.11\times10^{-14}\ \text{A},$$
$$I^{++}(0,e) = -0.15\times10^{-14}\ \text{A},$$
$$I^{++}(I,0) = +0.25\times10^{-14}\ \text{A},$$
$$I^{++}(I,e) = 3.00\times10^{-14}\ \text{A},$$
$$I_{\text{sig}}{}^{++}(I,e) = 3.01\times10^{-14}\ \text{A},$$
$$G = 0.547\ \text{cm}.$$

The measurements were taken at randomly varied electron-beam energies, ion-beam intensities, and electron-beam intensities. The results of these measurements are presented graphically in Fig. 1, and in tabular

* This work was partially supported by the Controlled Thermonuclear Research Program of the U. S. Atomic Energy Commission.
[1] W. C. Lineberger, J. W. Hooper, and E. W. McDaniel, preceding paper [Phys. Rev. 141, 151 (1966)].

TABLE I. Absolute cross sections for the single ionization of K^+ ions by electron impact.

Indicated electron energy, eV	Actual electron energy, eV	σ_{12} $\times 10^{17}$, cm^2	Random error, %	Maximum systematic error, %	Maximum total error, %
30	27±2	<0.15			
40	37±2	3.50	±10	±6	±16
45	42±2	5.12	±10	±6	±16
50	47±2	6.42	±10	±6	±16
60	57±2	7.16	±10	±6	±16
70	67±2	7.96	±10	±6	±16
80	77±2	8.22	±10	±6	±16
90	87±2	8.56	±10	±6	±16
100	97±2	8.56	±10	±6	±16
130	127±2	8.52	±7	±6	±13
150	147±2	8.26	±5	±6	±11
200[a]	197±3	7.52	±3	±6	±9
300	297±3	6.41	±3	±6	±9
400	397±3	5.41	±3	±6	±9
500[a]	497±3	4.69	±3	±6	±9
600	597±4	4.22	±3	±6	±9
700	697±4	3.76	±3	±6	±9
800	797±4	3.42	±3	±6	±9
900	897±4	3.16	±3	±6	±9
1000[a]	997±5	2.93	±3	±6	±9

[a] In addition to the usual continuous-beam measurements, the cross sections at these energies were measured while using the double beam pulsing scheme of Dolder, Harrison, and Thonemann, described in Appendix II. The pulsed-beam measurements agreed with the continuous-beam measurements to better than ±2% in each case.

form in Table I. The error brackets in Fig. 1 represent the "maximum total error" from Table I. Individual contributions to the total error are given in Table I.

The systematic errors, which are the same as those reported[1] in the Li^+ measurements, arise primarily from instrumentation calibration uncertainties; the systematic error is estimated to be a maximum of ±6% at all electron energies. The random error indicated at a particular electron energy is determined by the deviation from the mean cross section which is required to enclose all measured values at that particular energy. The total error, which the true error is believed not to exceed, is taken to be the sum of the random and systematic errors. The total error in the measurements is thus estimated to be ±9% above 150-eV electron energy. It increases at lower electron energies to ±16% at 37 eV. The root-mean-square error, which is not given in the table, ranges from ±7% at 1000 eV to ±12% at 40 eV.

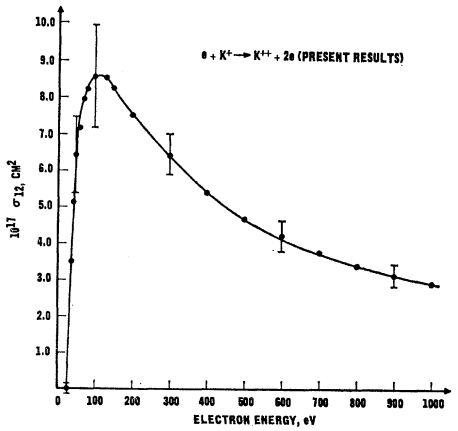

FIG. 1. Absolute cross sections for the single ionization of K^+ ions by electron impact.

In addition to these errors, there also exists some uncertainty in the mean electron energy in the interaction region. Retarding potential measurements show that the electron-energy spread is approximately ±2 eV about the mean energy. The mean electron energy was determined in the following manner. Both retarding potential measurements and measurements of the electron impact ionization of K^+ ions near threshold were not inconsistent with the assumption that the mean electron energy was about 3 eV less than the indicated energy. Furthermore, additional K^+ measurements (not presented here) indicate that the magnitude of this energy degradation must be less than 5 eV. An energy degradation of a few electron volts is typical of an oxide coated cathode. For these reasons, the mean electron energy in the interaction region is taken to be 3 eV less than the indicated energy; the electron energy has been accordingly corrected in the data presented here. The electron energy is considered to be uncertain by ±2 eV. This energy uncertainty has not been taken into account in determining the vertical error brackets. While the electron-energy uncertainty is insignificant at high energies, at low electron energies it must be considered. The uncertainty in the mean electron energy increases at higher energies, as a consequence of the 0.25% uncertainty in the indicated acceleration voltage.

All of the above data were taken while using the continuous-beam measurement technique described previously. In an attempt to assess the problems arising from pulsing the particle beams, cross-section measurements were also made at several electron energies while using the double beam pulsing scheme (described in Appendix II) of Dolder, Harrison, and Thonemann.[2] The beam pulsing rate was 1 kc/sec, and the ion- and electron-beam duty cycles were 50 and 40%, respectively. The pulsed-beam measurements were made at 200-, 500-, and 1000-eV electron energies. The pulsed-beam measurements agreed with the continuous-beam measurements in each case to better than ±2%. No systematic deviation from the continuous-beam results could be detected.

III. Na^+ RESULTS

The same apparatus and measurement techniques described above were used for the Na^+ measurements. Several natural varieties of sodium-rich feldspars were tested as a possible Na^+ emitting material. All of these materials exhibited an unacceptable level of K^+ emission, and it became necessary to employ a synthetically produced sodium-alumino-silicate, $Na_2O \cdot Al_2O_3 \cdot 2SiO_2$. This material was produced in the following manner. A mixture of reagent-grade Na_2CO_3, Al_2O_3, and SiO_2 in the appropriate ratio was made, and ground to 200 mesh size with a mullite mortar and pestle. To prepare

[2] K. T. Dolder, M. F. A. Harrison, and P. C. Thonemann, Proc. Roy. Soc. (London) **A264**, 367 (1961).

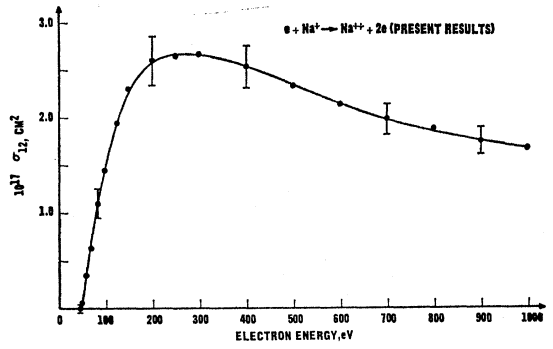

FIG. 2. Absolute cross sections for the single ionization of Na^+ ions by electron impact.

a filament, methanol was added to the mixture to form a slurry which could be painted onto the platinum gauze filament. The filament was then heated slowly to about 1500°C. This temperature was maintained for 10–15 min while the Na_2CO_3 was reduced to Na_2O thus forming the sodium-alumino-silicate. The mass spectra of the emitted ions indicated that within a few minutes after initial operation at 1000°C, Na^+ ions constituted 99.9% of the total ion emission.

The absolute cross sections for single ionization of Na^+ ions by electron impact were measured as a function of electron energy over the electron-energy range from below threshold (47.3 eV) to 1000 eV. The result of the consistency checks are essentially the same as those reported previously, and are not shown here. Measurements of the apparent cross section at electron energies below the threshold for formation of Na^{++} ions yielded a result which varied randomly between $\pm 0.04\times10^{-17}$ cm^2. The average of all below threshold measurements was 0.00×10^{-17} cm^2. The experimental results are shown graphically in Fig. 2, and in tabular form in Table II.

The random errors in the Na^+ measurements were somewhat smaller than those experienced in the K^+ measurements described previously. Since the systematic errors are the same as before, the total error is slightly reduced for the Na^+ measurements.

TABLE II. Absolute cross sections for the single ionization of Na^+ ions by electron impact.

Indicated electron energy, eV	Actual electron energy, eV	σ_{12} $\times10^{17}$, cm^2	Random error, %	Maximum systematic error, %	Maximum total error, %
45	42±2	<0.04			
60	57±2	0.34	±8	±6	±14
70	67±2	0.63	±8	±6	±14
85	82±2	1.10	±8	±6	±14
100	97±2	1.45	±8	±6	±14
125	122±2	1.94	±6	±6	±12
150	147±2	2.30	±5	±6	±11
200	197±3	2.60	±4	±6	±10
250	247±3	2.64	±4	±6	±10
300	297±3	2.67	±3	±6	±9
400	397±3	2.54	±3	±6	±9
500	497±3	2.33	±3	±6	±9
600	597±4	2.14	±2	±6	±8
700	697±4	1.99	±2	±6	±8
800	797±4	1.89	±2	±6	±8
900	897±4	1.77	±2	±6	±8
1000	997±5	1.69	±2	±6	±8

IV. COMPARISONS WITH THEORY AND EXPERIMENT

In this section, the Li^+, K^+, and Na^+ data are compared with the existing relevant theoretical and experimental data. There are presently no other experimental data available for the ionization of alkali ions by electrons and so no direct comparisons of the experimental results can be made. Moreover, no quantum-mechanical calculations for these systems are presently available. Thus the comparisons of these data must be made either with data for other atomic species or with "universal" electron-impact-ionization cross-section predictions. In either case such comparisons are most meaningful when made in terms of "reduced" cross sections, a term which is defined as follows.

Let σ_i be the cross section for electron impact ionization for a structure from states having ionization energy I. If ζ is the number of electrons in the shell from which the ionization takes place, then the reduced cross section for this process, $\hat{\sigma}_i$, is defined by

$$\hat{\sigma}_i = (1/\zeta)[I/I_H]^2\sigma_i, \tag{1}$$

where I_H is the ionization energy of atomic hydrogen, 13.60 eV. This definition is partially motivated by the investigations of Thomson,[3] who employed classical mechanics in his studies of electron impact ionization. The Thomson theory predicts that if

$$u = E/I, \tag{2}$$

where E is the energy of the incident electron, then $\hat{\sigma}(u)$ should be a universal function, valid for any element, whether ionized or neutral. Although the functional form predicted by the Thomson theory does not agree with either experimental observations or quantum-mechanical predictions, the concept of a "universal" ionization curve appears to have some approximate validity, a fact which has been observed by Elwert[4] and others.[5,6] It is found that if reduced ionization cross sections for a number of elements are plotted as a function of u, then a single curve can be drawn which agrees with all of the experimental data to within about a factor of 2.

Drawin[5] has proposed an empirical formula for electron-impact-ionization cross sections, based upon the concept of the universal ionization curve. The Drawin formula reads

$$\hat{\sigma}(u) = 2.66 f_1[(u-1)/u^2]\ln[1.25 f_2 u]\pi a_0^2, \tag{3}$$

where f_1 and f_2 are two arbitrary constants which may

[3] J. J. Thomson, Phil. Mag. **23**, 449 (1912).
[4] G. Elwert, Z. Naturforsch. **7a**, 432 (1952).
[5] H. W. Drawin, Z. Physik **164**, 513 (1961).
[6] M. J. Seaton, Planet. Space Sci. **12**, 55 (1964).

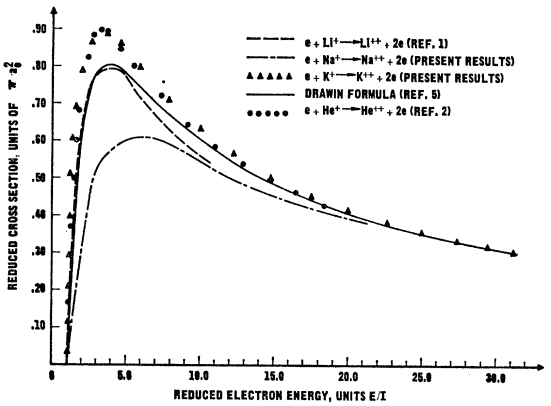

FIG. 3. Comparison of the experimental results for the ionization of Li^+, K^+, and Na^+ ions by electron impact with empirical and classical predictions.

depend on the ionization process under consideration. If no information on the process is known, then f_1 and f_2 should be taken to be unity. The Drawin formula approaches a $(\ln u)/u$ functional form as u increases; in this respect it is consistent with the Born approximation predictions. Drawin considers his formula to be uniformly valid over the entire electron-energy range. The Drawin empirical formula is plotted with f_1 and f_2 equal to unity in Fig. 3. Also shown in this figure are the reduced Li^+, Na^+, and K^+ cross sections, together with the reduced He^+ cross sections of Dolder *et al.*[2] The reduced cross sections are obtained under the assumption that all of the ejected electrons come from the least tightly bound states ($1s$ for Li^+, $2p$ for Na^+, and $3p$ for K^+). Although such an assumption is valid for He^+ and Li^+, there will be some s-shell contributions to the Na^+ and K^+ measurements. Consideration of this component would lower these reduced cross sections by 5–10%, an amount which is not significant in a comparison of this type. It is seen that all of the curves are similar, with Na^+ perhaps 40% lower than the others at low reduced impact energies.

Burgess and Rudge[7,8] have calculated the cross sections for the ionization of hydrogenic positive ions by electron impact in the Coulomb-Born-Oppenheimer approximation. They find that the reduced cross sections $\hat{\sigma}(u)$ for all the hydrogenic ions approach the same analytic form, in the limit of large electron impact energy. In this limit the effects of the different nuclear Coulomb fields of the several hydrogenic ions become insignificant. The scaling relation suggested by the Thomson theory appears to be valid for hydrogenic positive ions in the limit of large electron energies. The He^+ calculations of Burgess and Rudge[7,8] approach the experimental He^+ results of Dolder, Harrison, and Thonemann[2] at the highest electron energies attained, while overestimating the cross sections at lower energies, in the manner typical of Born approximation calculations.

The Dolder, Harrison, and Thonemann reduced He^+ cross sections agree closely at high electron energies with the reduced H-atom electron-impact-ionization cross sections measured by Fite and Brackmann.[9] The hydrogen atom and the helium ion are, of course, adjacent members of the hydrogen-like isoelectronic sequence. It is also of interest to compare the reduced cross sections for electron impact ionization of the alkali ions with those for the isoelectronic noble gases. If the scaling procedure is valid for other than hydrogenic ions, then the reduced cross sections for isoelectronic structures should approach each other in the limit of high electron impact energies. The question of s-shell contributions in the scaling of, say, K^+ and Ar is not important, as the relative s-shell contributions should be almost the same in either case. It should be noted that the absolute alkali ion cross sections are obtained without recourse to pressure measurements. Figure 4 compares the reduced Li^+ cross section with the reduced He total[10] cross section of Smith[11] and the very recent He measurements of Rapp,[12] who used an "effusive-flow" technique to determine pressure. At the highest electron energies attained, the reduced Li^+ data and the reduced He results of Smith coincide. The measurements of Rapp lie approximately 4% above the Li^+ data. The McLeod gauge correction that Rapp obtains in this case is *plus* 4%.

In Fig. 5, the reduced K^+ cross sections are compared to the cross sections for formation of Ar^+, using the total cross section data of Smith[11] and Rapp.[12] The Ar^+ cross sections were obtained in each case by multiplying

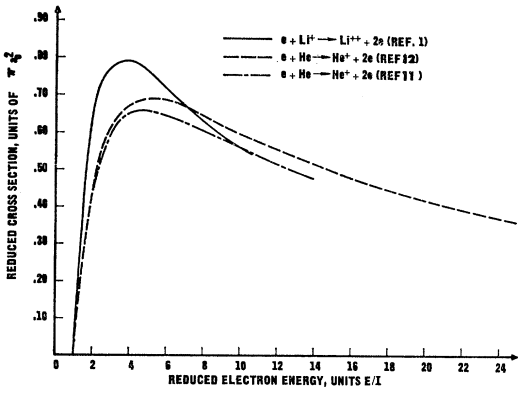

FIG. 4. Comparison of the experimental results for the ionization of Li^+ ions by electron impact with the experimental results of others for the ionization of He and He^+ by electron impact.

[7] A. Burgess, Astrophys. J. **132**, 503 (1960).
[8] A. Burgess and M. R. H. Rudge, Proc. Roy. Soc. (London) A273, 372 (1963).

[9] W. L. Fite and R. T. Brackmann, Phys. Rev. **112**, 1141 (1958).
[10] The comparison should be made with the cross sections for formation of He^+, but, since the number of He^{++} ions formed is less than ½% of the total, σ_T is nearly equal to σ_1.
[11] P. T. Smith, Phys. Rev. **36**, 1293 (1930).
[12] D. Rapp and P. Englander-Golden (private communication, to be published).

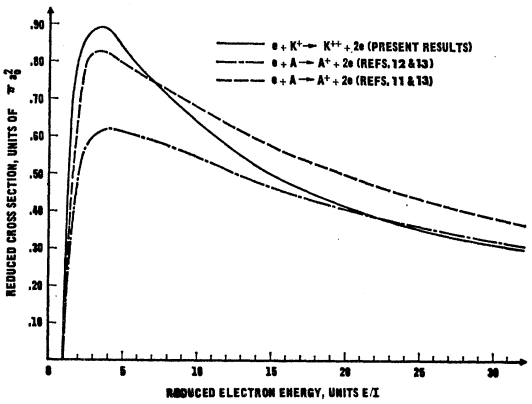

FIG. 5. Comparison of the experimental results for the ionization of K^+ ions by electron impact with the experimental results of others for the ionization of Ar by electron impact.

the total cross sections by the σ_1/σ_T abundance ratios determined by Bleakney.[13] The reduced K^+ data and the reduced Ar^+ data of Rapp are virtually coincident at high electron energies. The McLeod gauge correction in the Rapp measurements was minus 12%.

Figure 6 depicts the comparison between the reduced Na^+ data and the reduced total Ne ionization data of Smith[11] converted by use of the σ_1/σ_T ratios of Bleakney.[13] Neon is the one simple gas which deviates substantially from the "universal" cross-section predictions. The Na^+ and Ne results do not approach each other in the high-energy limit; it appears that the mechanism which gives rise to the unusual behavior of Ne is operative to a much smaller extent in the isoelectronic Na^+ ion. The Ne data of Rapp[12] are similar to those of Smith and are not shown.

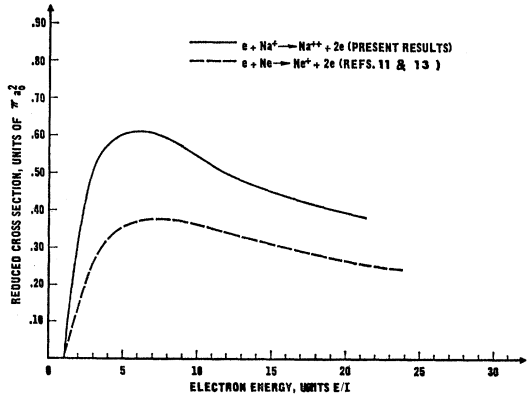

FIG. 6. Comparison of the experimental results for the ionization of Na^+ ions by electron impact with the experimental results of others for the ionization of Ne by electron impact.

[13] W. Bleakney, Phys. Rev. 36, 1303 (1930).

ACKNOWLEDGMENT

We are pleased to acknowledge the assistance of Professor E. W. McDaniel for helpful discussions throughout the accumulation of these data, the interpretation of the results, and the preparation of this manuscript.

APPENDIX I: DERIVATION OF σ_{12} IN TERMS OF EXPERIMENTAL PARAMETERS

In this section an expression for the cross section for single ionization of ions by electron impact will be developed in terms of experimentally observed parameters. With obvious modifications this expression can be utilized for any crossed-beam experiment. Before the development can proceed it is necessary to define a collision cross section.

Consider a parallel beam of monoenergetic projectiles approaching the origin of the laboratory coordinate system, as shown in Fig. 7. The beam is traveling parallel to the x-y plane, but is inclined at an angle θ to the y axis. The beam is uniformly composed of particles of number density n particles/cm^3 and speed V cm/sec in the laboratory frame of reference. Let N_p be the total number of these projectiles which pass through a 1-cm^2 area in the x-z plane per second. The particle flux and the number density are related as follows:

$$N_p = nV\cos\theta. \tag{4}$$

Consider N_t targets to be located in that region of the x-z plane through which the projectile beam passes. We assume that there are sufficiently few targets present to ensure that none is shielded by another and that no projectile interacts with more than one target. We further assume that the interactions do not remove any of the targets, so that N_t will remain constant. The cross section for a particular projectile-target inter-

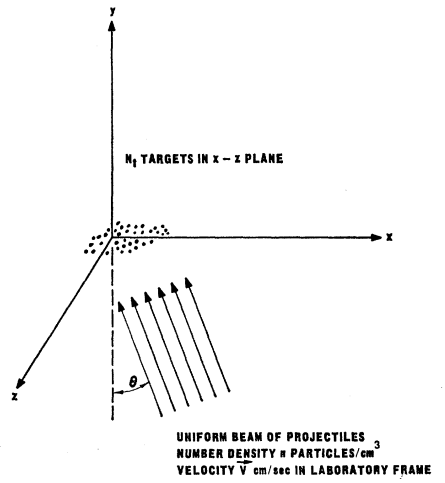

FIG. 7. The laboratory coordinate system in which the ionization cross section will be defined.

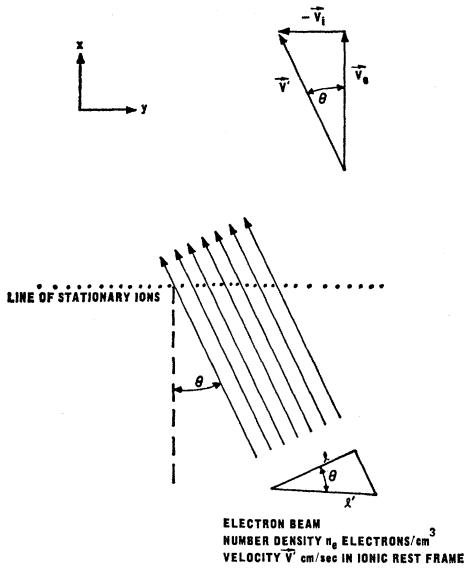

FIG. 8. View of the collision region in the ionic rest frame at a given instant of time. The ion and electron velocities in the laboratory frame are $\mathbf{V}_i$ and $\mathbf{V}_e$, respectively.

action "r" can now be defined. It is apparent that the number of interactions r occurring per second, R, is directly proportional to both N_p and N_t. Inserting a constant of proportionality σ, we may write

$$R=\sigma N_p N_t. \tag{5}$$

This expression is the defining relation for σ, the cross section for interaction r.

With the aid of this definition, the cross section for the single ionization of ions by electron impact can now be developed. Consider a rectangular xyz coordinate system in the laboratory frame of reference. Let a monoenergetic uniform beam of ions traveling in the $+y$ direction be intersected normally by a monoenergetic uniform beam of electrons traveling in the $+x$ direction. The ion and electron velocities are $\mathbf{V}_i$ and $\mathbf{V}_e$ cm/sec, respectively, in the laboratory frame of reference. The physical extent of the ion beam is over $0\leq z\leq h$ and $0\leq x\leq w$, while that of the electron beam is over $0\leq z\leq h$ and $0\leq y\leq l$. If the total electron current is J amperes, then the number density in the electron beam is given by

$$n_e=(J/lheV_e)\text{electrons/cm}^3, \tag{6}$$

where e is the magnitude of the electronic charge. In order to phrase this problem in such a form that Eq. (5) is applicable, it will be necessary to transform the problem to a frame of reference in which one of the particle beams is stationary. Since $V_e\gg V_i$ in general, we shall transform to a frame in which the ion beam is stationary. This new frame will be referred to as the ionic rest frame.

Following this transformation, the collision region appears, at a given instant of time, as shown in Fig. 8. In this frame the electron beam is traveling upward and to the left with velocity $\mathbf{V}'$ cm/sec; consequently any reacted targets are effectively replenished, while the total number of ions in the path of the electron beam N_t remains constant. Since multiple interactions do not occur as a result of the tenuous nature of the ion beam, the ion beam width w is neglected and the ions are shown in a linear array. The geometry of this transformed system is one in which Eq. (5) is directly applicable.

In the ionic rest frame, the electrons have a velocity $\mathbf{V}'$ cm/sec, whose magnitude is given by the equation

$$V'=(V_e^2+V_i^2)^{1/2}\text{ cm/sec}. \tag{7}$$

The electron number density n_e, however, remains invariant under the transformation to the ionic rest frame. The number of electrons per second crossing unit area in the plane of the ions is seen to be

$$N_p=\frac{n_eV'l}{l'}=\frac{J}{ehl'}\frac{V'}{V_e}, \tag{8}$$

where use has been made of Eq. (6) in obtaining Eq. (8). As is evident from Fig. 8, the length l' is the projection of l on the stationary line of ions.

The total number of ions N_t present in that portion of ion beam through which the electron beam is passing at any given instant is given by

$$N_t=(I^+/e)(l'/V_i)\text{ ions}, \tag{9}$$

where I^+ is the total ion current. The interaction of interest here is the single ionization of ions; the total number of reactions per second is given by

$$R=(I^{++}/2e)\text{ ionizing collisions/sec}, \tag{10}$$

where I^{++} is the total current of doubly ionized particles produced by electron impact. The factor of 2 arises as a result of the double charge on these ions. Equations (8), (9), and (10) may now be substituted directly into Eq. (5); following this substitution, and some simplification, we obtain

$$\frac{I^{++}}{h}=2\sigma_{12}\frac{V'}{eV_iV_e}\frac{I^+}{h}\frac{J}{h}. \tag{11}$$

It is noted that each of the beam currents appearing in this equation is divided by the height of that beam; each of these quotients thus has dimensions of a *linear* current density. Equation (11), however, applies only to the highly idealized case of uniform beams of the same height. If we now consider ion and electron beams whose linear current densities are functions of z, then, to a first approximation, Eq. (11) is valid for any small segment, say z to $z+h$, of the nonuniform beams. If h is allowed to approach zero, the quotients in Eq. (11) become linear current densities, and Eq. (11) can be

rewritten as

$$i^{++}(z)=2\sigma_{12}(V'/eV_iV_e)i^{+}(z)j(z), \qquad (12)$$

valid for all z, and for beams whose current densities are nonuniform in z. The lower case i and j represent linear current densities. Integrating Eq. (12) and noting that the coefficient of $i^{+}(z)j(z)$ is not a function of z, we obtain

$$\int_{-\infty}^{\infty} i^{++}(z)dz=2\sigma_{12}\frac{V'}{eV_eV_i}\int_{-\infty}^{\infty} i^{+}(z)j(z)dz. \qquad (13)$$

The left-hand side of Eq. (13), however, is the total doubly ionized signal current I^{++}. Using this result, together with Eq. (7), and solving for σ_{12}, we finally obtain

$$\sigma_{12}=\frac{eV_iV_e}{2[V_i^2+V_e^2]^{1/2}}\frac{I^{++}}{\int_{-\infty}^{\infty} i^{+}(z)j(z)dz} \qquad (14)$$

which is the desired result.

APPENDIX II: BEAM-PULSING SCHEMES

Whereas this experiment primarily utilized continuous ion and electron beams, there exist several beam-pulsing schemes which might have been employed in the measurements. It is of interest therefore to consider, for the case of experiments of the type described here, these various pulsing schemes, and to compare them to the continuous-beam technique. Such a comparison will be made in the remainder of this Appendix.

The primary detrimental effects occurring in the beam intersection region are the space-charge interactions of the beams, and the background pressure resulting from turning one beam off and on. It is to these effects that the measurement techniques must address themselves. In order to facilitate this comparison, measurements of the following hypothetical event will be compared using the various measurement schemes. This event is the single ionization of ions by electron impact at a particular ion and electron energy. Continuous ion and electron currents of 1.0×10^{-7} A and 1.0×10^{-3} A, respectively, are assumed to produce 0.5×10^{-15} A of doubly ionized ions as a result of electron-impact ionization. The 1.0×10^{-7} A ion beam produces a noise current at the doubly ionized particle detector of 1.0×10^{-15} A; this current is composed both of doubly ionized ions which have been produced by charge stripping on the background gas, and of stray singly ionized ions which have reached the doubly ionized particle detector. The continuous-beam measurement will be considered first, followed by the pulsed-beam measurements.

Continusus Beams

Since continuous-beam measurements have already been discussed in detail,[1] only the pertinent conclusions will be presented here. The continuous-beam measurement assumes that the ionization signal current is given by the difference between I^{++} with ion and electron beams on and I^{++} with only the ion beam on. Since the presence of the electron beam increases the chamber pressure, the charge-stripped portion of the I^{++} noise current is larger when the electron beam is on than it is when the electron beam is off. The measured ionization signal current is thus too large by the amount of this increase. In order for this error to be small, it is generally necessary that the experiment be performed in an ultra-high vacuum environment. This pressure-dependent error is shown to be not serious if continuous-beam measurements at electron energies below the ionization threshold energy yield apparent cross sections which are insignificant compared with those obtained well above threshold. In addition to this pressure-dependent error, the deflection of ions by the space charge of the electron beam may cause the noise current to the doubly ionized particle detector to change in the presence of the electron beam. Thus electron-beam space-charge effects can also produce a measurement error. Measurements below threshold can again be utilized to determine whether the magnitude of such an error is significant.

If such errors were not present, then the continuous-beam measurement should yield the correct ionization signal current. The measured ratio of the ionization signal to ion-beam noise (SNR) would be given by

$$\mathrm{SNR}=\frac{I^{++}(I,e)-I^{++}(I,0)}{I^{++}(I,0)}$$

$$=(1.5\times10^{-15}-1.0\times10^{-15})/1.0\times10^{-15}=0.5.$$

Pulsed Beams

If a particle beam is pulsed on and off with a period much less than the vacuum chamber time constant, the system pressure does not change appreciably from an "on" cycle to an "off" cycle, but rather the system assumes an average pressure. The advantage of all beam-pulsing schemes over the continuous-beam measurements lies in the fact that it is possible to allow the vacuum system to attain an average steady pressure. Thus an increase in charge-stripped currents resulting from pressure changes need not be a source of error.

Typical pulsing rates are on the order of a few kilocycles per second. At this rate the length of one pulse of beam particles is typically far greater than the size of the experimental apparatus. Thus the pulsed beam in the apparatus must not be thought of as a series of short beam segments; rather, a continuous beam of particles is either filling the apparatus, or it is not. As a consequence of these beam-pulse lengths, the

effects of the electron space charge mentioned in connection with continuous-beam measurements are still present in all beam-pulsing schemes. Thus, for experiments of this type, whenever the base pressure is sufficiently low and pressure changes do not present significant source of error, the continuous-beam measurement technique is equal to or better than any pulsed-beam measurement technique.

The possible beam-pulsing schemes include pulsed ion beams, pulsed electron beams, and pulsed ion and electron beams. These cases will be considered separately and compared to the continuous-beam measurements by means of the hypothetical experiment described previously. The question naturally arises as to how the intensities of the pulsed and continuous beams should be related, in order to obtain the most meaningful comparisons between pulsed- and continuous-beam measurements. The comparisons could be based on either the peak currents or the mean currents being equal in the measurement schemes being compared. Since the magnitude of the electron-beam space-charge convergence effect is determined by the magnitude of the electron current during the time at which both beams are present in the interaction region, the comparisons in all cases are based on this peak electron current, rather than the mean current, being equal.

Pulsed Electron Beam

A schematic diagram depicting the various particle currents in the case of a pulsed electron beam is presented in Fig. 9(a). It is noted that the desired ionization signal, shown in crosshatch, is present as a time-varying component on a steady background. Sufficient information is present to extract this component, provided that either the I^{++} current can be measured as a function of time, or phase-sensitive detection techniques can be applied. Unfortunately the 10^{-15} A

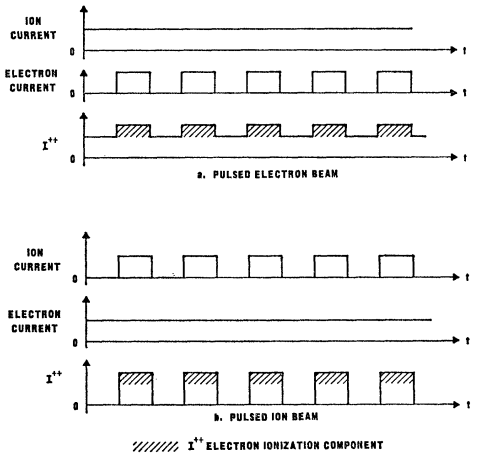

FIG. 9. Current wave forms applicable to pulsed-electron-beam experiments and to pulsed-ion-beam experiments.

level of this signal is smaller than the present technological capabilities of phase-sensitive detectors. It would, however, be possible to measure the I^{++} signal current using a multiplier as a particle counter and appropriately gating the particle pulses to two scalers. The difference in the count rate of the two scalers would then represent the desired signal. The use of a multiplier, however, introduces the additional uncertainty of the efficiency of the multiplier. The converging effects of the electron-beam space charge, if significant, will give rise to a nonelectron-impact ionization current which is in phase with the electron-beam pulses. Thus, if such space-charge effects are present, they will give rise to a measurement error, such as occurred in the case of the continuous-beam measurements.

Pulsed Ion Beam

The appropriate waveforms for the case of a pulsed ion beam are shown in Fig. 9(b). It is apparent that there is insufficient information present to separate the electron-impact-ionization current from the ion-beam noise current. Thus this case need be considered no further.

Pulsed Ion and Electron Beams

The crossed-beam experiments of Dolder, Harrison, and Thonemann[2,14,15] utilized pulsed ion and electron beams, in the manner shown in Fig. 10(a). The ion beam is pulsed at 5 kc/sec, with a 50% duty cycle, while the electron beam is pulsed at the same frequency, but with a 25% duty cycle.[16] The pulsing frequency is sufficiently high to ensure a steady pressure in the vacuum chamber. The phase of the electron is adjustable with respect to that of the ion beam, thus giving rise to coincidence and anticoincidence modes of operation. In the anticoincidence mode, an ion current flows only when the electrons are cut off, and the I^{++} current consists only of the ion beam noise component. In the coincidence mode the electron beam crosses the interaction region only when ions are present, and the resulting I^{++} current contains both electron-ionization and noise components. The difference in the *mean* current levels in these two modes is a measure of the electron-impact-ionization component; the fact that the desired signal information is contained in the *mean* current levels is the principal advantage of this pulsing scheme. Since only mean current levels are of importance, a sensitive instrument such as the vibrating capacitor electrometer may be employed for the measurements.

[14] K. T. Dolder, M. F. A. Harrison, and P. C. Thonemann, Proc. Roy. Soc. (London) **A274**, 546 (1963).
[15] K. T. Dolder, M. F. A. Harrison, and P. C. Thonemann, Proc. Roy. Soc. (London) **82**, 368 (1963).
[16] The duty cycle for one of the beams should be less than 50% in order to avoid beam synchronization difficulties.

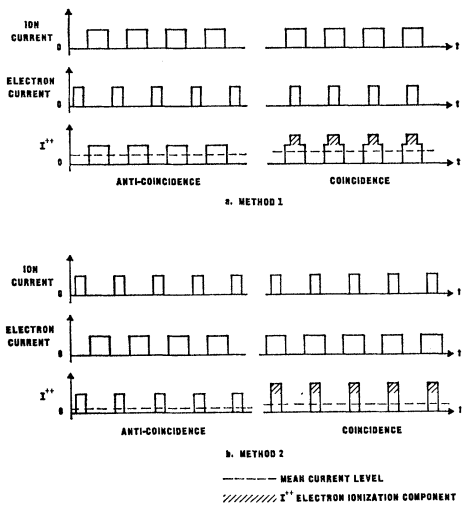

FIG. 10. Current wave forms applicable when both ion and electron beams are pulsed.

Using the parameters of our hypothetical experiment we evaluate the signal-to-noise ratio as follows:

$$\begin{aligned}\text{SNR} &= (I_c^{++} - I_{ac}^{++})/I_{ac}^{++}, \\ &= (0.625\times10^{-15} - 0.50\times10^{-15})/0.50\times10^{-15}, \\ &= 0.25,\end{aligned}$$

where I_c^{++} and I_{ac}^{++} are the mean I^{++} currents in the coincidence and anticoincidence modes, respectively. This SNR is a factor of 2 worse than that obtained with continuous beams under similar conditions; in addition the I^{++} currents which must be measured are a factor of 2 smaller in magnitude than in the continuous-beam case.

A second coincidence-anticoincidence measurement is possible if the duty cycles of the ion and electron beam are interchanged. The pulse shapes for this arrangement are shown in Fig. 10(b). The mode of operation is the same as before and the SNR is calculated to be

$$\begin{aligned}\text{SNR} &= (I_c^{++} - I_{ac}^{++})/I_{ac}^{++}, \\ &= (0.375\times10^{-15} - 0.25\times10^{-15})/0.25\times10^{-15}, \\ &= 0.5.\end{aligned}$$

The SNR is seen to be equal to that obtained in the continuous-beam measurements, but the current levels are lower by a factor of 4.

The choice as to which of these two pulsing schemes is better depends upon the experiment being performed. In the hypothetical measurement used for comparison, there was no stray signal current from the electron beam. If, however, both the ion and electron beams produced stray signal currents, then the best SNR would be obtained by allowing the noisier beam to have the shorter duty cycle. The overriding consideration in the choice, however, may well be the shape of the beam pulses. If one beam pulse is much less uniform than the other, then the less uniform beam should have the shorter duty cycle.

In both of these pulsing schemes the converging effect of the electron beam is the same as it would be in the continuous-beam case. The effect of electron-beam space charge in any event must still be assessed. The fact that the I^{++} current levels in the pulsed-beam measurements are lower than those in the continuous-beam measurements is a direct result of constraining the peak electron-beam space-charge product to be constant throughout the comparisons. This constraint is reasonable since the upper limit on usable electron-beam intensities (and hence the upper limit for the SNR) is set by space charge.

Conclusions

The following principal conclusions, pertinent to experiments of the type described here, can be drawn from this discussion.

(1) The continuous-beam measurements are superior to any pulsed-beam measurements, provided that the base pressure is sufficiently low and that pressure changes are not significant during the measurement process.

(2) Pulsing only the electron beam can provide useful measurements if a sufficiently sensitive phase-sensitive detector is available or if a multiplier is used in a pulse counting mode.

(3) The desired signal information cannot be obtained if only the ion beam is pulsed.

(4) Pulsing both ion and electron beams permits determination of the desired signal while requiring only measurement of *mean* current levels.

(5) The effect of electron-beam space charge on the ion beam noise current is not assessed in any of these measurement schemes. This effect must still be considered before reliable measurements can be made.